Resonance Effects in the Interaction of NLS Solitons with Potential Wells

K.T. Stoychev, M.T. Primatarowa and R.S. Kamburova

Institute of Solid State Physics

Bulgarian Academy of Sciences,

1784 Sofia, Bulgaria

Abstract

The interaction of nonlinear Schrödinger (NLS) solitons with potential wells with variable shapes is investigated numerically. For fixed initial velocities below the threshold for transmission, the outcome pattern as a function of the width of the potential yields periodically repeating regions of trapping, transmission and reflection. The observed effects are explained by an excitation and a following resonant deexcitation of amplitude (shape) oscillations of the solitons at the boundaries of the well, associated with radiation modes.

Self-localized nonlinear waves (solitons) have been studied in many areas of physics including optics, solid state, molecular, plasma, elementary particles etc. Within integrable models, solitons exhibit remarkable stability - they propagate with constant velocities and shapes and emerge from collisions unchanged except for phase and space shifts. Real physical systems are often described by nonintegrable equations or such containing nonintegrable perturbations. This leads to inelastic soliton interactions with a variety of outcomes. As solitons provide an important mechanism for energy and information transport in nonlinear systems, such interactions have attracted considerable attention (see i.e. Ref. 1 for a review of earlier works on soliton dynamics in nearly integrable systems). Investigations have been focussed on collisions between solitons in nonintegrable models and interactions of solitons with defects and inhomogeneities. In both cases, due to the inelasticity of the interactions, solitons can change their velocities, break into a number of localized and dispersive waves and/or be trapped into bound states. In addition, interesting resonance phenomena have been observed.

Resonace effects in kink-antikink collisions have been studied numerically in some nonintegrable equations including ϕ^4, double and modified sine-Gordon and others [2, 3, 4]. For initial velocities below the threshold for trapping, a sequence of narrow regions of reflection have been obtained. These reflection windows have been explained by a "two-bounce" resonance mechanism involving excitation of an internal shape mode during the first collision, temporal trapping of the solitons due to loss of kinetic energy, deexcitation of the shape mode during the second (backward) collision and escape of the kinks to infinity (reflection). The resonance condition requires that the time between the two collisions is commensurate with the period of the shape mode. Fine three- and four-bounce resonance structures have also been obtained [5]. Collisions of vector NLS solitons have been investigated in [6] where fractal resonant patterns have been obtained.

Similar effects have been observed in the interactions of solitons with impurities. The latter break the translational symmetry of the unperturbed system and create an effective potential for scattering or capture of the solitons [1]. Resonance effects in the kink-impurity interaction have been investigated in [7, 8, 9]. It has been shown in particular that kinks can be reflected by an attractive impurity via a "two-bounce" resonance mechanism, analogous to that of kink-antikink interaction involving the excitation and deexcitation of a localized impurity mode [8], or an impurity and a shape mode [9]. Scattering of NLS solitons from

point defects has been studied in [10, 11, 12] involving a variety of nonresonant outcomes.

A problem of considerable theoretical and practical importance is the interaction of solitons with extended defects [13, 14, 15, 16]. Trapping of solitons in potential wells and nonclassical behavior for kinetic energies close to the height of potential step have been obtained in [16], but no resonance phenomena have been observed. The investigations however have been restricted to potential widths comparable to the soliton width. In the present work we investigate in detail the dynamics of bright NLS solitons impinging on potential wells with variable shapes. For fixed initial velocities slightly below the threshold for transmission, the increase of the width of the well yields alternating regions of capture and transmission, and occasionally - narrow reflection windows. The regions of transmission, capture and reflection follow a remarkable periodicity. The observed effects are explained by excitation and a following resonant deexcitation of amplitude (shape) oscilations of the soliton at the boundaries of the well. These oscillations are not associated with true internal shape modes of the soliton, but with dispersive radiation modes.

As a model in our numerical simulations we used the discrete nonlinear Schrödinger equation which describes the dynamics of nonlinear Bose-type excitations in atomic or molecular chains in the presence of defects which change locally the energy:

$$i\frac{\partial \alpha_n}{\partial t} = -(\alpha_{n+1} + \alpha_{n-1} - 2\alpha_n) - 2 \mid \alpha_n \mid^2 \alpha_n + d_n \alpha_n \,. \tag{1}$$

In the continuum limit corresponding to wide solitons (compared to the lattice constant) it turns into a perturbed NLS equation:

$$i\frac{\partial \alpha}{\partial t} + \frac{\partial^2 \alpha}{\partial x^2} + 2 \mid \alpha \mid^2 \alpha = d(x)\alpha \,. \tag{2}$$

For $d(x) \equiv 0$ (2) possesses a fundamental bright soliton solution:

$$\alpha(x,t) = \frac{1}{L}\mathrm{sech}\frac{x - vt - x_0}{L} e^{i(vx/2 - \omega t)} \,, \quad \omega = \frac{v^2}{4} - \frac{1}{L^2} \,, \tag{3}$$

where L and v are the width and the velocity of the soliton.

It is well known, that for $d_n = 0$ (1) is a nonintegrable discretization of the completely integrable continuum NLS equation. For sufficiently wide solitons however, the discreteness-induced effects are negligible, and the solution (3) is stable on ideal discrete lattices. We

checked numerically the stability of (3) with $L \geq 4$ for very long time intervals. Thus (3) was input as initial condition in the simulations, placed 50 sites away from the defect region to avoid radiation losses due to overlapping. A predictor-corrector method [17] was used, periodic boundary conditions and chains much longer than the defect region in order to eliminate boundary effects. The accuracy of the calculations was controlled through the conservation of the norm (number of particles), which is better than 10^{-6}.

The total energy associated with the solution (3) on an ideal lattice is:

$$E_s = \int_{-\infty}^{\infty} (\mid \frac{\partial \alpha}{\partial x} \mid^2 - \mid \alpha \mid^4) \, dx = \frac{v^2}{2L} - \frac{2}{3L^3} \, , \tag{4}$$

where the first term describes the kinetic energy of the free quasiparticles, and the second term - the nonlinear energy responsible for the formation of the soliton. The evolutionary pattern depends in general on the interplay between these two energies and the energy of interaction with the defects E_d

$$E_d = \int_{-\infty}^{\infty} d(x) \mid \alpha \mid^2 \, dx \tag{5}$$

The effects studied below correspond to the most interesting case of slow solitons with kinetic energy of the order of the energy of interaction with the defect and large nonlinear energy:

$$E_{kin} \sim |E_d| \ll |E_{int}|$$

or equivalently:

$$v^2 L^2 \sim 2|d|L \ll 1 \, . \tag{6}$$

The large nonlinear energy is required to preserve the integrity of the soliton during the interaction.

Scattering of bright NLS solitons from single point defects has been studied in detail in [10, 11, 12]. The corresponding interaction energy when the soliton is on top of the defect is:

$$E_d = d \int_{-\infty}^{\infty} \delta(x) \mid \alpha \mid^2 \, dx = \frac{d}{L^2} \tag{7}$$

When $E_{kin} \gg |E_d|$, the solitons are not influenced considerably by the defect, and for $E_{kin} \ll |E_d|$ the solitons are reflected even by an attractive defect. The possible outcomes

in the case of slow solitons ($E_{kin} \sim |E_d|$) and moderate defect strengths are transmission or capture. No resonance reflection windows have been obtained. A natural question arises as to what happens when the defect spreads over several lattice sites. The energy of interaction with N consecutive defects when the soliton is in the middle of the defect region is:

$$E_d = d \int_{-N/2}^{N/2} \mid \alpha \mid^2 \, dx = \frac{2d}{L} \tanh \frac{N}{2L} \tag{8}$$

One can expect, that for a small number of defects, ($N \leq L$), the evolution should be similar to this of a soliton interacting with a single defect with N-times greater strength. This turns out to be true only for kinetic energies much smaller than the interaction energy. In the case of comparable energies, the delocalization of the defect (which decreases the interaction energy) can change the evolution from capture to transmission (Fig. 1). It is worth noting that the sharper the defect - the stronger the radiation accompanying the interaction.

The focus of the present study lies in the interaction of NLS solitons with potential wells considerably wider than the soliton width. We modelled rectangular potential wells by N equal consecutive defects with $d = -0.007$ and used solitons in the form (3) with widths $L = 5.75$, which are stable on an ideal lattice. For initial velocities $v < 0.04$ the solitons are trapped inside the well and for $v > 0.06$ they pass through it and escape to infinity. For initial velocities in the intermediate region, the outcome pattern as a function of the width of the well exhibits periodically alternating regions of transmission and capture, and occasionally, at the boundaries between them - narrow reflection windows. This is shown on Fig. 2 where we have plotted the final velocity of the soliton as a function of the width of the well for different values of the initial velocity. When trapped, the soliton oscillates back and forth inside the well with zero average velocity which we have plotted as final. The sharp minima with negative final velocity ($v_f < 0$) correspond to reflection. These reflection "windows" are extremely sensitive to the initial velocity. The relative widths of the regions of transmission and capture depend on the initial velocity and can be quite different, but the period of repeat remains constant and depends weakly on the velocity.

Fig. 3 illustrates the evolutionary patterns corresponding to capture, transmission and reflection. It is clearly seen, that amplitude (shape) oscillations are excited when the soliton enters the potential well and persist while the soliton is inside the well. Whenever the soliton leaves the defect region, the shape oscillations are almost totally extinguished. This brings

forward the explanation of the observed resonance phenomena: when the soliton reaches the defect region it interacts inelastically with the sharp boundary and looses part of its kinetic energy exciting additional modes. These can be internal shape modes of the soliton and/or dispersive modes (radiation). We can distinguish between them by examining the frequency of the shape oscillations. The frequencies of the true internal shape modes can be obtained by adding small perturbation $\alpha_1(x,t) = \varphi_1(x)e^{-i\Omega t}$ to the unperturb solution (3) and solving the linearized Schrödinger equation for it:

$$\frac{\partial^2 \varphi_1}{\partial x^2} + (\Omega + \frac{4}{L^2 \cosh^2(x/L)})\varphi_1 = 0\,. \tag{9}$$

The frequencies of the shape mode determined from (9) are $\Omega_1 = -0.0735$ and $\Omega_2 = -0.00094$. The period of the amplitude oscillations obtained from the numerical data on Fig. 3 is T=208 which yields a frequency of $\Omega = -2\pi/T = 0.030$. It practically coincides with the internal frequency of the unperturbed soliton (3) $\omega = -0.0296$. Shape oscillations with the internal soliton frequency have been reported in [18] and are explained by interference of the soliton with radiation modes with twice the soliton frequency. This shows that similarly to the case of collision of vector solitons [6], the amplitude oscillations which we observe are due to radiation, emitted during the inelastic interaction of the soliton with the boundary, and not to true internal shape modes. The soliton crosses the defect region accompanied by the radiation and this configuration is stable and weakly damped. When the soliton meets the second boundary, different outcomes are possible depending on the timing. In the general case, as the initial velocities are very small, the reduced kinetic energy of the soliton is not sufficient to overcome the potential barrier of the second boundary, the soliton is reflected from it and eventually gets trapped. However, the interaction of the soliton with the boundary is phase-sensitive and if the time for which the soliton crosses the defect region is commensurate with the period of the shape oscillations, the inelastic interaction with the second boundary can extinguish the shape oscillations, adding their energy back to the kinetic energy of the translational motion and allowing the soliton to overcome the barrier and escape to infinity which leads to transmission. The higher the initial velocity of the soliton - the wider the transmission regions (Fig. 2). In some cases the resonant condition for escape is achieved after the soliton has crossed the defect region twice - in the forward and backward directions. This yields the observed narrow reflection windows which are analogous to the three-bounce resonances observed in [5]. Due to the radiation losses

accompanying the propagation of the soliton inside the well, these higher-order resonances are very sharp, extremely sensitive to the initial velocity and difficult to observe.

The interaction energy when the soliton is at the boundary of the defect region is:

$$E_d = d \int_0^N \mid \alpha \mid^2 \, dx = \frac{d}{L} \tanh \frac{N}{L} \tag{10}$$

For narrow potential wells, comparable to the soliton width, the interaction energy is smaller, leading to weaker shape oscillations and a narrower region of trapping. For sufficiently wide potential wells ($N \gg L$, $\tanh(N/L) \sim 1$), when the soliton does not "feel" the second boundary, the interaction energy and the excited shape oscillations are constant, which results in the observed periodic outcome pattern. For very wide potential wells, due to the radiation losses accompanying the oscillating soliton, the regions of transmission get narrower and eventually close down.

An increase of the depth of the well leads to wider regions of trapping and narrower regions of transmission (Fig. 4), while the total period remains unchanged. The inelastic interaction of the soliton with the boundary is stronger in this case and a larger portion of the kinetic energy of the soliton is transformed into radiation. A more exact resonance condition is required at the second boundary for the escape of the soliton, which yields narrower regions of transmission.

Contrarily, the change of the shape of the potential well from rectangular to trapezoid leads to wider transmission regions and narrower regions of capture (Fig. 5). The potential in this case is smoother and the perturbation it induces is weaker. Hence a smaller portion of the kinetic energy is transformed into radiation and the resonance condition at the second boundary is more relaxed.

We also checked the dependence of the evolutionary pattern on the initial position of the soliton with respect to the boundary of the defect region. For an initial soliton in the form (3) and a fixed velocity $v = 0.05$ we obtain a threshold initial distance of 15 lattice sites, above which the soliton passes through the defect region and below it gets trapped. This can be explained by the radiation losses when the initial unperturbed soliton overlaps with the defect region. The chaotic behavior of the outcome with the initial soliton position obtained in [16] can be attributed to the different type of coupling between the soliton and the shape mode.

Acknowledgments

This work is supported in part by the National Science Foundation of Bulgaria under Grant No. F911.

---

[1] Yu.S. Kivshar and B.A. Malomed, Rev. Mod. Phys. **61**, 763 (1989).

[2] M.J. Ablowitz, M.D. Kruskal and J.R. Ladik, SIAM J. Appl. Math. **36**, 478 (1979).

[3] D.K. Campbell, J.F. Schonfeld and C.A. Wingate, Physica **9D**, 1 (1983).

[4] M. Peyrard and D.K. Campbell, Physica **9D**, 33 (1983).

[5] D.K. Campbell and M. Peyrard, Physica **18D**, 47 (1986).

[6] J. Yang and Yu Tan, Phys. Rev. Lett. **85**, 3624 (2000).

[7] Yu.S. Kivshar, Zhang Fei and L. Vázquez, Phys. Rev. Lett. **67**, 1177 (1991).

[8] Zhang Fei, Yu.S. Kivshar and L. Vázquez, Phys. Rev. A **45**, 6019 (1992).

[9] Zhang Fei, Yu.S. Kivshar and L. Vázquez, Phys. Rev. A **46**, 5214 (1992).

[10] Yu.S. Kivshar, A.M. Kosevich and O.A. Chubykalo, Zh. Eksp. Teor. Fiz. **93**, 968 (1987) [Sov. Phys. JETP **66**, 545 (1987).

[11] Yu.S. Kivshar, A.M. Kosevich and O.A. Chubykalo, Phys. Lett. A **125**, 35 (1987).

[12] X.D. Cao and B.A. Malomed, Phys. Lett. A **206**, 177 (1995).

[13] R. Sharf and A.R.Bishop, Phys.Rev. A **46**, R2973 (1992).

[14] J.J.-L. Ting and M. Peyrard, Phys. Rev. E **53**, 1011 (1996).

[15] H. Frauenkron and P. Grassberger, Phys. Rev. E **53**, 2823 (1996).

[16] G. Kälbermann, Phys. Lett. A **252**, 37 (1999).

[17] L.F. Shampine and M.K. Gordon, *Computer Solution of Ordinary Differential Equations* (Freeman, San Francisco,1975).

[18] M. W. Chbat, J. P. Prucnal, M. N. Islam, C. E. Soccolich and J. P. Gordon, J. Opt. Soc. Am. B **10**, 1386 (1993).

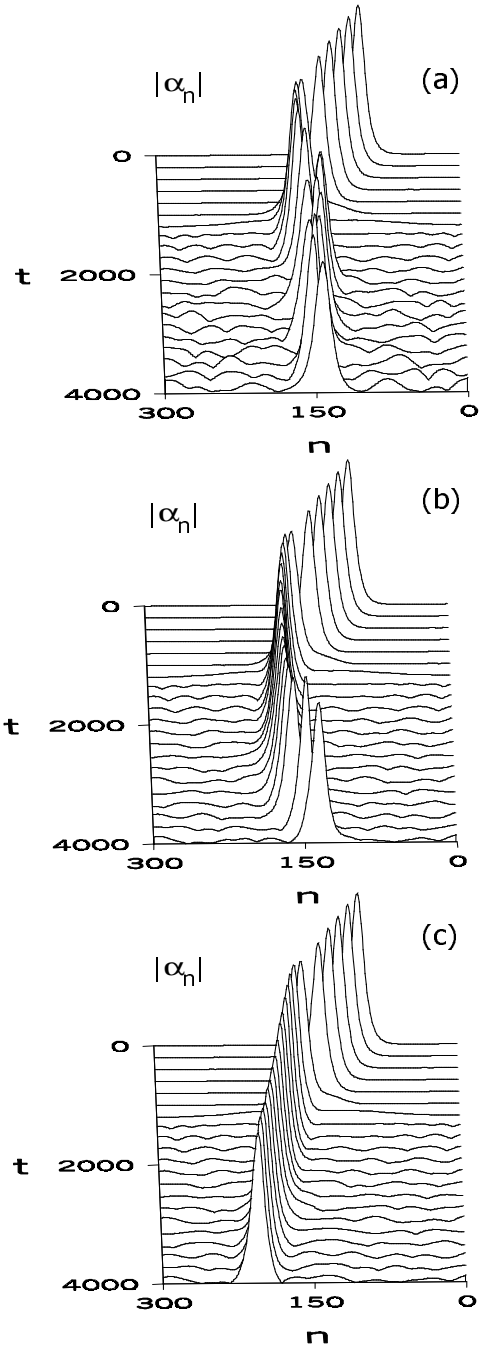

FIG. 1: Soliton interaction with a small number of impurities for $v = 0.05$. (a) $N = 1$, $d = -0.035$; (b) $N = 2$, $d = -0.0175$; (c) $N = 3$, $d = -0.0117$. (a) and (b) correspond to capture and (c) - to transmission.

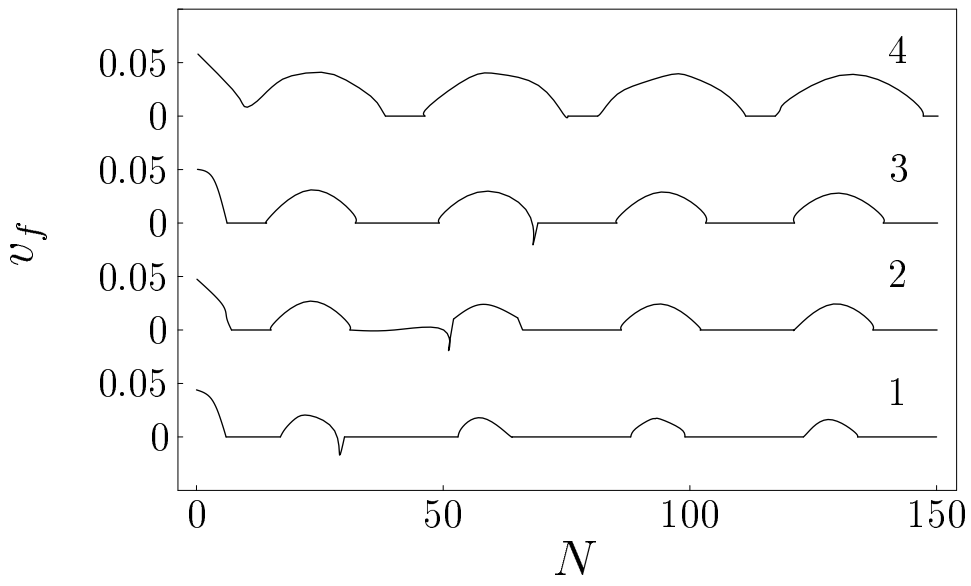

FIG. 2: Final soliton velocity v_f for $d = -0.007$ and different initial velocities v. Curves 1 to 4 correspond to $v = 0.0440$; 0.0476; 0.0502 and 0.0580 respectively.

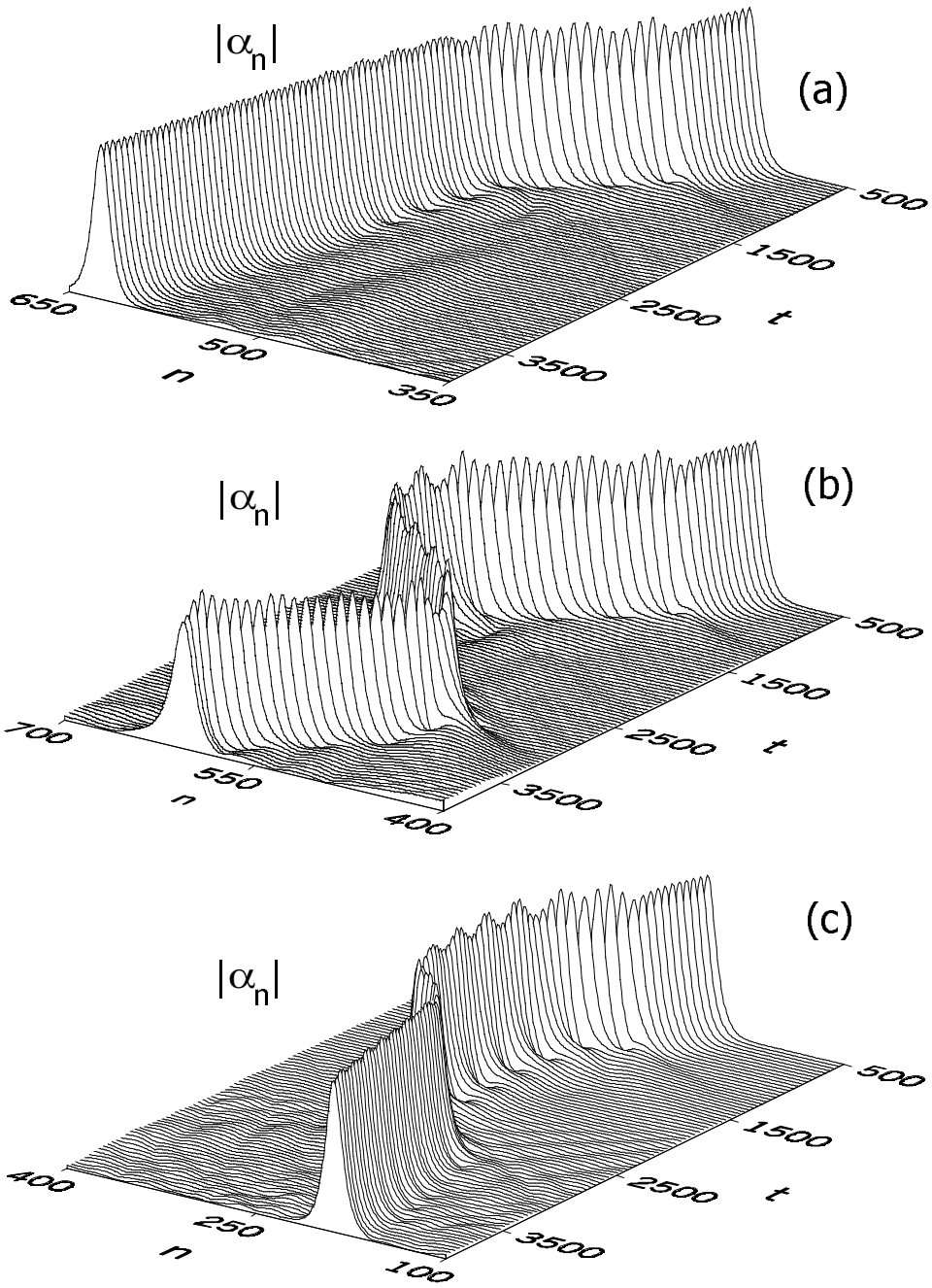

FIG. 3: Outcome patterns for $v = 0.05$, $d = -0.007$ and different number N of defects. (a) $N = 95$ - transmission, (b) $N = 110$ - trapping and (c) $N = 33$ - reflection. Only a portion of the chain around the defect region is presented, while the the total length of the chain exceeds 10 potential widths (to avoid boundary effects).

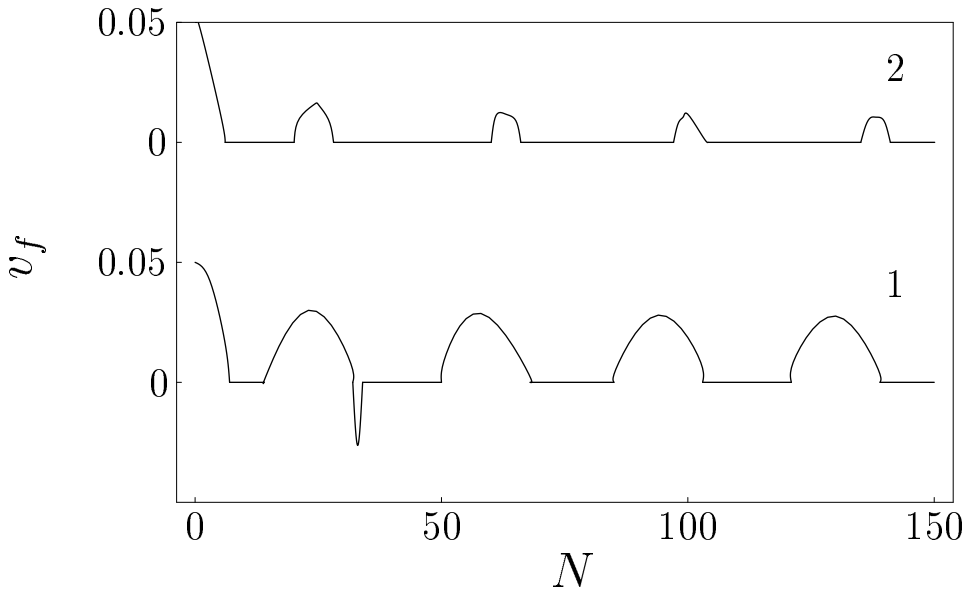

FIG. 4: Final soliton velocity v_f for $v = 0.05$ and different depths of the potential well; curve 1 - $d = -0.007$ and curve 2 - $d = -0.008$.

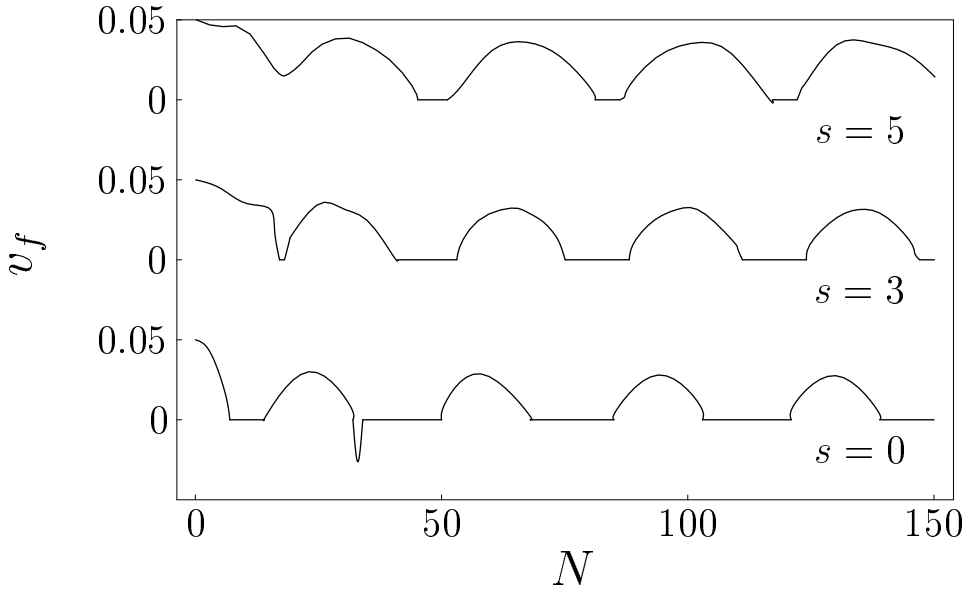

FIG. 5: Final soliton velocity v_f for $v = 0.05$, $d = -0.007$ and trapezoidal potential wells with different slope (s is the extension of the slope).